Structure−Activity Analysis of Anandamide Analogs: Relationship to a Cannabinoid Pharmacophore†

Brian F. Thomas,*,‡ Irma B. Adams,§ S. Wayne Mascarella,‡ Billy R. Martin,§ and Raj K. Razdan||

Research Triangle Institute, Research Triangle Park, North Carolina 27709, Medical College of Virginia/Virginia Commonwealth University, Richmond, Virginia 23298, and Organix, Inc., Woburn, Massachusetts 01801

Received July 17, 1995⊗

Anandamides are endogenous fatty acid ethanolamides that have been shown to bind to the cannabinoid receptor and possess cannabimimetic activity yet are structurally dissimilar from the classical cannabinoids found in *Cannabis sativa*. We have employed molecular dynamics studies of a variety of anandamides to characterize their conformational mobility and determine whether there are pharmacophoric similarities with Δ^9-THC. We have found that a looped conformation of these arachidonyl compounds is energetically favorable and that a structural correlation between this low-energy conformation and the classical cannabinoids can be obtained with the superposition of (1) the oxygen of the carboxyamide with the pyran oxygen in Δ^9-THC, (2) the hydroxyl group of the ethanol with the phenolic hydroxyl group of Δ^9-THC, (3) the five terminal carbons and the pentyl side chain of Δ^9-THC, and (4) the polyolefin loop overlaying with the cannabinoid tricyclic ring. The shape similarity is extended to show that other fatty acid ethanolamides that possess varying degrees of unsaturation also vary in their conformational mobility, which affects their ability to overlay with Δ^9-THC as described above. Within this series of compounds, the most potent analog, the tetraene (arachidonyl) analog (i.e., anandamide itself), was determined to have restricted conformational mobility that favored an optimal pharmacophore overlay with Δ^9-THC. Eight pharmacologically active anandamide analogs are shown to have similar conformational mobility and pharmacophore alignments that are conformationally accessible. Furthermore, when these compounds are aligned to Δ^9-THC according to the proposed pharmacophore overlay, their potencies are predicted by a quantitative model of cannabinoid structure−activity relationships based solely on classical and nonclassical cannabinoids with a reasonable degree of accuracy. The ability to incorporate the pharmacological potency of these anandamides into the cannabinoid pharmacophore model is also shown to support the relevance of the proposed pharmacophore model.

Introduction

Anandamide (*cis*-5,8,11,14-eicosatetraenoylethanolamide; Figure 1) is a naturally occurring fatty acid ethanolamide initially isolated from porcine brain and shown to bind to the cannabinoid receptor and produce cannabinoid effects.[1] Subsequently, anandamide has been shown to inhibit cAMP production via the G-protein-coupled cannabinoid receptor[2,3] and to produce a combination of cannabinoid behavioral effects in mice[4−6] and rats.[7] Since the identification of anandamide as an endogenous cannabimimetic, a number of additional endogenous fatty acid ethanolamides,[8] as well as esters of fatty acids,[9] have been reported to bind to cannabinoid receptors. The identification of these endogenous compounds and the recent synthesis of a wide variety of anandamide analogs[6,9,10] represent a significant expansion in the diversity of cannabimimetics.

Traditional cannabinoid structure−activity relationships (SAR) indicate that the molecular requirements for cannabinoid activity include (1) the phenolic hydroxyl, (2) the lipophilic side chain, and (3) an appropriately oriented carbocylic ring system.[11−15] However, in 1981, Milne and Johnson[16] demonstrated that a shape similarity and heteroatom alignment existed between prostaglandins and the THC analog 9β-hydroxy-11-nor-Δ^9-HHC. Their prostaglandin overlap theory led to the development of the extremely potent nonclassical cannabinoids[17] and subsequently to the discovery of the cannabinoid receptor.[18] Although a great deal of investigation has been centered on the cannabinoid pharmacophore, little has been described regarding the ability of eicosanoids to be accommodated by the SAR described for classical cannabinoids.

As illustrated in Figure 1, the structures of anandamides differ greatly from the tricyclic structure of classical cannabinoids (e.g., Δ^9-THC). The substantial differences between the two classes of compounds militate against the existence of any simple structural correlation that can explain their pharmacological similarity and provide a reasonable starting point for the comparison of other analogs. Because the cannabinoid receptor's structure and shape are still being characterized and no crystallographic data are available showing receptor-bound ligand, there is little direct knowledge regarding the nature of a particular ligand's interaction with the receptor. Therefore, it is only possible to derive a pharmacophore model based on a structural comparison of active and inactive molecules that provides a consistent explanation of the observed

† Abbreviations: THC, tetrahydrocannabinol; SAR, structure−activity relationships; HHC, hexahydrocannabinol; rms, root mean square; QSAR, quantitative structure−activity realtionships; CoMFA, comparative molecular field analysis; PLS, partial least-squares; MEP, molecular electrostatic potential.

* Address all correspondence to Dr. Brian F. Thomas, Center for Chemistry and Life Sciences, Research Triangle Institute, P.O. Box 12194, Research Triangle Park, NC 27709-2194. Tel: (919) 541-6552 (voice). Fax: (919) 541-6499.

‡ Research Triangle Institute.

§ Medical College of Virginia/Virginia Commonwealth University.

|| Organix, Inc.

⊗ Abstract published in *Advance ACS Abstracts,* December 15, 1995.

0022-2623/96/1839-0471$12.00/0

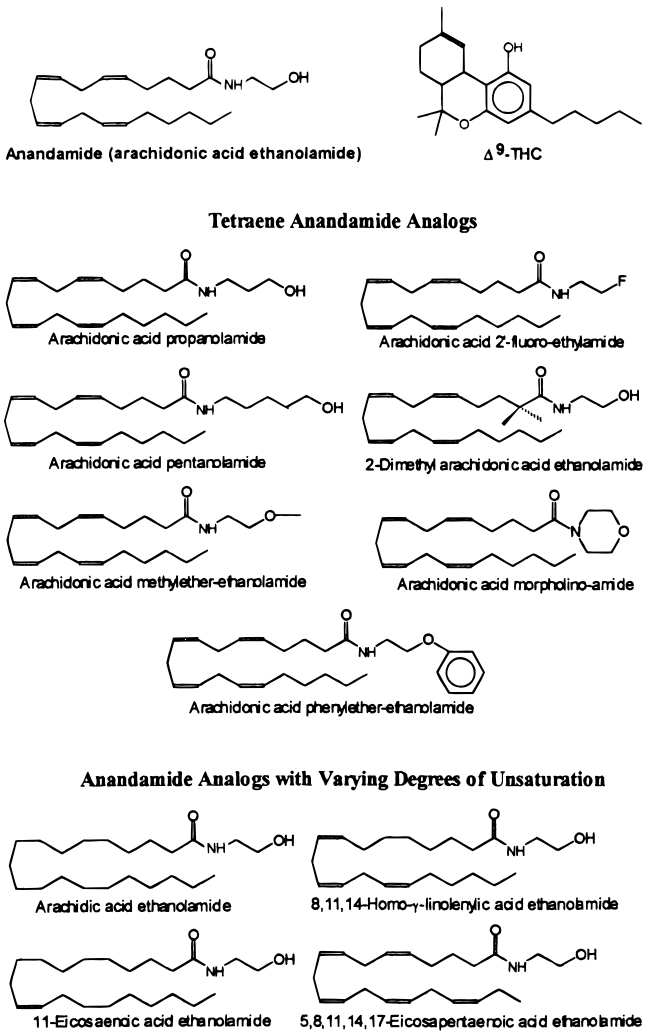

Figure 1. Structures of anandamide analogs and Δ^9-THC.

data. Ideally, this model should be predictive and facilitate the design of novel compounds of greater potency or selectivity.

In this report, low-energy conformations of anandamide-like compounds were determined by molecular dynamics simulations and shown to allow superposition of analogous pharmacophore groups within these compounds and Δ^9-THC. The proposed conformation of anandamide is supported by previous studies on the conformational mobility of arachidonic acid[19] as well as evidence that arachidonic acid adopts a similar conformation during self-epoxidation reactions.[20,21] In the conformation described here for anandamide, electronegative regions associated with the hydroxyl and carbonyl oxygen atoms can be superimposed with similar electronegative regions in Δ^9-THC, as can linear hydrocarbon side chains and π-electron rich regions. The ability to attain an analogous shape and orientation of electronegative regions is shown to be dependent on the degree of unsaturation in the fatty acid chain, with the tetraene chain allowing optimal molecular alignment with Δ^9-THC. The pharmacophore model is shown to be consistent with the preexisting cannabinoid SAR and to provide a rational comparison of anandamide analogs such that the variation in potency among a series of eight anandamide analogs is accurately predicted. The successful incorporation of anandamides into the preexisting cannabinoid SAR provides a predictive environment capable of facilitating the design and testing of novel compounds.

Methods

Molecular Models and Energy Minimization. All molecular modeling and molecular dynamics simulations were carried out on a Silicon Graphics Indigo ^{2}XZ or Silicon Graphics Iris 4D/310 VGX workstation with SYBYL molecular modeling software (v 6.03, Tripos, Inc., St. Louis, MO). An initial structure of anandamide was generated from the molecular fragments provided within SYBYL for arachidonic acid and ethanolamine. Anandamide analogs were modeled by modification of this basic structure. Electrostatic charges for all of the analogs were calculated on the basis of the method of Gasteiger−Huckel. After energy minimization using the SYBYL force field had progressed to a point where the difference in energy between successive iterations was <0.01 kcal/mol, each analog was subjected to molecular dynamics simulations. Gasteiger−Huckle-derived charges were used for all dynamics simulations and QSAR analyses. Semiempirical calculations were performed using SPARTAN (WaveFunction, Inc., CA) in order to further compare the electrostatic properties of anandamide and Δ^9-THC.

Molecular Dynamics. Molecular dynamics runs were performed in order to evaluate the conformational mobility of the compounds. Molecular dynamics runs were simulated at 100, 200, 300, and 400 K for 1 ps each and finally allowed to remain at 500 K for 100 ps. Once the molecule had reached 500 K, snapshots of its conformation were taken at 1 ps intervals, resulting in 100 separate conformations being obtained. After the molecular dynamics runs had concluded, each recorded conformation was subjected to energy minimization as described above until the difference in energy between successive iterations was <0.01 kcal/mol, resulting in a set of "quenched" conformations that were stored for further examination.

Alignment of Anandamides to Δ^9-THC. An automated fitting procedure was used to minimize the root mean square (rms) deviation between five atoms in the anandamide analogs and five analogous atoms in Δ^9-THC according to the superposition shown in Figure 2A. These atoms were selected on the basis of the importance of the pharmacophore groups in Δ^9-THC, particularly the phenolic hydroxyl and the pyran oxygen (electronegative regions) and the lipophilic side chain. This set of analogous atoms could be used in most of the molecules involved in this study; however, if no appropriate atom was present in the anandamide analog (e.g., the 2′-fluoroanandamide has no phenolic proton), only four atoms were used in the rms procedure. The rms procedure, while holding each conformation rigid, places it in space so as to overlay the five atoms as closely as possible to the five template atoms in Δ^9-THC. The rms deviation was recorded for each conformation. After the molecules had been so aligned, the molecular volume of Δ^9-THC was subtracted from the molecular volume of the various conformations.

Relationship between Conformational Mobility and Pharmacophoric Conformation. The relationship between conformational mobility and ability to overlap with Δ^9-THC was evaluated by plotting the energies of the conformations obtained for each anandamide analog against the rms deviation and volume difference. The first variable, the rms deviation obtained during the rms-fitting procedure of each conformation to Δ^9-THC, indicates the distance differences between the atoms used in the superposition. The second variable, the volume difference, quantitates the unique, nonoverlapping volume of each conformation in its particular alignment.

Constraint of Tetraene Anandamide Analogs to Pharmacophoric Conformations. The ability of a series of tetraene-based anandamide analogs (Figure 1) to form pharmacophore-overlapping conformations of low energy was evaluated by constraining the polyene chain up to and including the carbonyl (in the identical conformation as shown for anandamide in Figure 2A) and also constraining the appropriate pharmacophore atoms to the distances found for their

respective atoms in Δ^9-THC. Energy minimizations (to <0.01 kcal/mol steps) on the fully constrained molecules were followed by further minimizations after removal of the distance constraints (again to <0.01 kcal/mol steps). Finally, the entire molecule was energy minimized with no constraints in order to find the local energy minimum conformation that most closely overlays the pharmacophore. This strategy forced any conformational changes that occurred during energy minimization to occur in the region where the substituent modifications were made (i.e., the ethanolamide region).

Prediction of the Pharmacological Potencies of Tetraene Anandamide Analogs. In order to evaluate the pharmacophoric conformation chosen for anandamides, a three-dimensional QSAR model based on classical and nonclassical cannabinoids[15] was used to predict the potency of the tetraene analogs. Initially, the CoMFA analysis[15] was repeated with the following modifications: (1) the probe atom (sp^3 carbon with a +1 charge) was positioned at lattice points spaced around the molecules at 1 Å increments, as opposed to the 2 Å spacing performed previously; (2) the cross-validation was done using a "leave-one-out" procedure that allows comparison between different partial least-squares (PLS) analyses.

All analogs were constrained to the pharmacophoric conformation as described above and then overlayed with respect to anandamides polyene chain (up to and including the carbonyl oxygen) so as to maximize their conformational overlay with anandamide while allowing the various substituents to be compared. After their alignment, the steric and electrostatic properties of each analog were determined so that their activity could be predicted by the CoMFA QSAR model. The logarithm of the actual ED_{50} was plotted against the logarithm of the predicted ED_{50} and analyzed using least-squares linear regression.

Rederivation of the CoMFA QSAR Model and Inclusion of Tetraene Anandamide Analogs. After the initial QSAR analysis based on 33 classical and nonclassical cannabinoids, the eight tetraene anandamide analogs were incorporated into the cannabinoid QSAR model and the analyses were repeated (behavioral data taken from Adams et al.[6]). In all instances, cross-validated PLS analysis was run to determine the optimal number of components in the model and to evaluate the robustness of the model. During these analyses, any CoMFA column whose standard deviation was <2.0 was excluded to shorten computation time. The number of components was increased as long as the cross-validated r^2 increased, up to a maximum of five components. The number of cross-validation groups was chosen so that one compound was omitted from the training set, and the resulting equation was used to predict the behavioral potency of the omitted compound. The process was repeated, leaving out a different compound, until each compound had been excluded and predicted exactly once (a leave-one-out PLS analysis). The resulting individual squared errors of prediction were summed to give the predictive residual sum of squares (PRESS). The PRESS was compared to the standard deviation of the actual potencies to obtain a cross-validated q^2. Once the optimal number of components had been determined through cross-validation, the number of components was set to that value and the number of cross-validation groups was set to zero. The analysis performed with these parameters is the *final* analysis wherein the model derived is based on all compounds in the training set.

Comparison of CoMFA Fields. The steric and electrostatic features of the QSAR analysis were graphically depicted by plotting the product of the standard deviation of the CoMFA column data and the PLS coefficients. This plot produces an enhanced view of the pharmacophore model where the steric and electrostatic properties that are correlated with the observed differences in pharmacological potency are visualized three-dimensionally. The plots are color-coded so that contours in blue indicate areas where steric bulk of analogs is strongly associated with increased predicted potency and contours in cyan are also associated with areas of increased potency but to a lesser degree than those in blue. Areas contoured in orange, on the other hand, are areas where steric bulk is associated with decreased predicted potency but to a lesser extent than contours in red. The electrostatic forces associated with changes in potency were contoured so that negative charge should be moved away from areas contoured in orange and red and closer to areas in cyan and blue, assuming that a more potent analog is desired. The steric and electrostatic contour plots were derived for the pharmacological potency in each behavioral assay, with and without the inclusion of the eight tetraene anandamide analogs, in order to allow comparisons to be made among the various pharmacophores.

Results

Alignment of Anandamides to Δ^9-THC. The conformation of anandamide, which served as the basis for defining the pharmacophoric alignment, is shown in stereoviews after it has been aligned to Δ^9-THC (Figure 2B). These stereoviews emphasize the overall shape similarity and the similar spacing of the oxygen atoms, as well as the close proximity of the carbonyl oxygen atom and the C14 double bond. The close proximity of these two structural features appears to be energetically favorable in arachidonic acid[19] and also appears to be an important conformation in solution.[20]

When anandamide and Δ^9-THC are overlayed, subtraction of the molecular volume of each compound from the other allows the visualization of their unique molecular volumes (Figure 2C). In these views, one can see that the overall shape of Δ^9-THC is closely mimicked by this conformation of anandamide. Furthermore, it appears that the molecular volume of this particular conformation of anandamide (contoured in green) is confined to regions that would be predicted to permit pharmacological activity (i.e., there does not appear to be anandamide volume at the C9–C11 position that has previously been associated with decreased cannabinoid potency[13,15,22]). This is seen in Figure 2C by the absence of green contours penetrating into the red or orange contours. The red/orange and blue/cyan contours were derived from our originalCoMFA SAR study[15] and indicate regions where steric volume is associated with decreased or increased biological potency, respectively.

With regard to the electrostatic properties of each compound, Figure 2D reveals the similarity between the electrostatic potential of anandamide and Δ^9-THC. These molecular electrostatic potential (MEP) contours were generated using semiempirical calculations based on the AM1 Hamiltonian (SPARTAN, WaveFunction, Inc.) to derive the partial charges and contour maps. There is a striking similarity in the electronegative regions (red) between Δ^9-THC and anandamide in the proposed pharmacophoric conformation. The electronegative regions at the "bottom" of the molecule (pyran and carbonyl in Δ^9-THC and anandamide, respectively) suggest potential sites for hydrogen bonding with a receptor site, as could the electronegative region at the top. Thus, the MEP maps reflect the similarity in two of the three points chosen for superposition, with the remainder being associated with the hydrophobic side chain.

Relationship between Conformational Mobility and Pharmacophoric Conformation. The relationship between conformational mobility of anandamide analogs with zero, one, three, four, and five double bonds in their polyene chains and their ability to overlap with Δ^9-THC was evaluated by plotting the energies of the conformations obtained for each analog against the rms fit and volume difference defining the pharmacophore

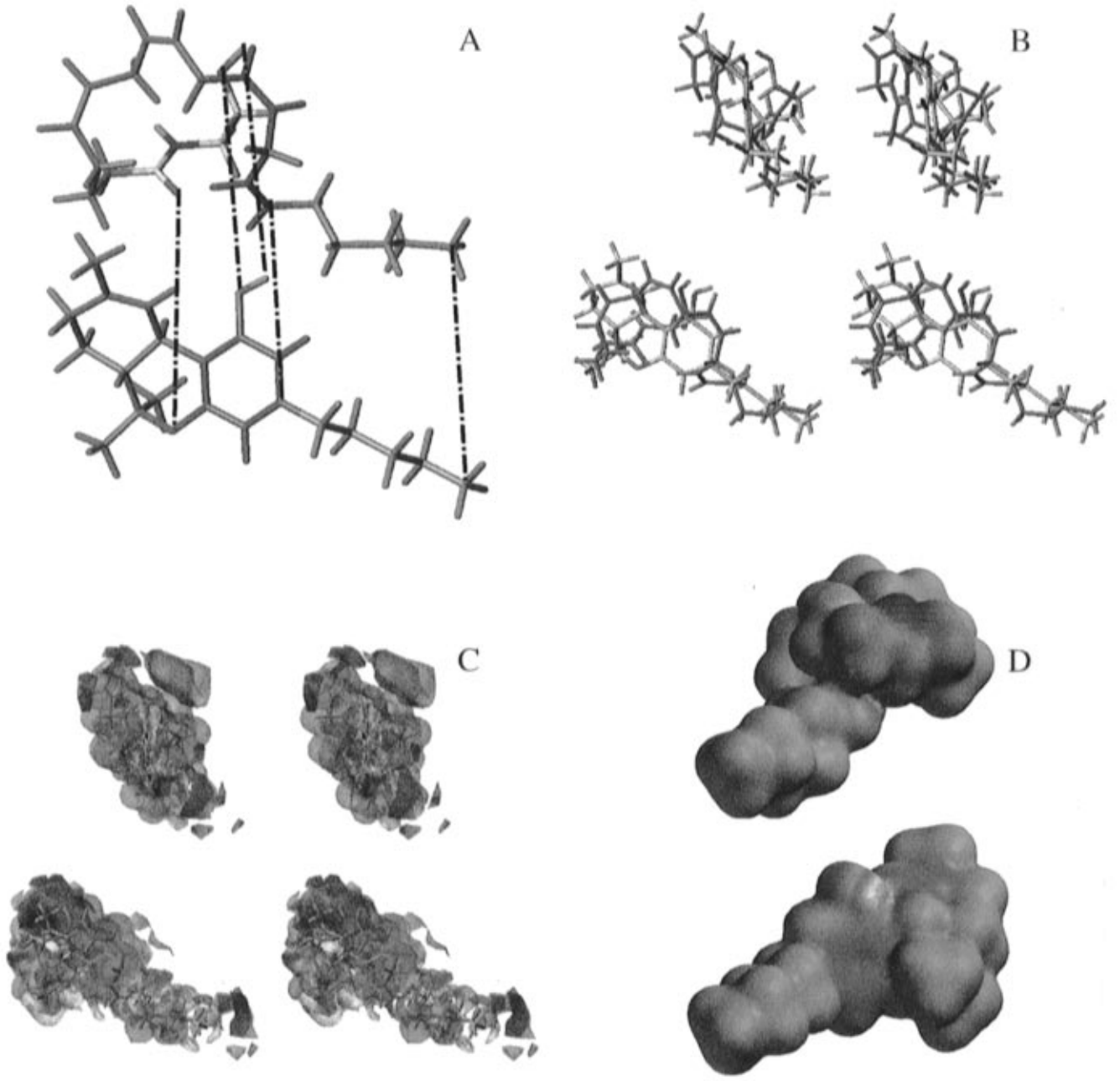

Figure 2. Structural comparisons of anandamide and Δ^9-THC. (A) Alignment used for comparing fatty acid ethanolamides to Δ^9-THC (bottom structure). The dashed lines show the five atoms used for superposition by rms fitting. Although in this figure the superpositioned atoms are shown for anandamide (top), these same atoms were used in all of the fatty acid ethanolamides. The atoms of each structure have been colored so as to emphasize their structural similarity. (B) Stereoviews of the overlayed structures of Δ^9-THC (yellow carbon atoms) and anandamide (green carbon atoms). (C) Stereoviews of the overlayed structures of Δ^9-THC (yellow carbon atoms) and anandamide (green carbon atoms) showing their nonoverlapping molecular volumes contoured around them in yellow (unique volume of Δ^9-THC) and green (unique volume of anandamide). The contoured areas in red and blue were derived from a QSAR analysis (Thomas et al., 1991) and indicate areas where steric bulk leads to decreased predicted potency (red) or increased predicted potency (blue) in a cannabinoid test of spontaneous locomotor activity. (D) Relative electrostatic potentials of anandamide (top) and Δ^9-THC (bottom) color-coded onto a constant electron density (95%) surface. The electrostatic potential scale ranges from -75 (red) to $+35$ (blue). Note that in this view the molecules have been rotated so that the side chains are on the left.

overlap (Figure 3). The rms deviation has been scaled from 0 to 10 in all graphs, and the color coding indicating volume difference is equivalent for all plots, allowing the graphs to be more readily compared. Upon close inspection of these graphs, it is clear that the conformations obtained with an anandamide analog with no double bonds (i.e., arachidic acid) have greater rms deviations, as well as greater unique molecular volumes when overlayed with Δ^9-THC (Figure 3A), than molecules with double bonds in their structures. Furthermore, the degree of rms deviation decreases in a systematic fashion as the number of double bonds in the hydrocarbon side chain increase from zero to five. This is shown by the shift in the data points to the left (lower rms difference) from the widely scattered pattern of points obtained with arachidic acid (Figure 3A), to the less scattered plots obtained with the analogs with one double bond (11-eicosaenoic acid ethanolamide; Figure 3B), three double bonds (homo-γ-linolenylic acid ethanolamide; Figure 3C), and four double bonds (anan-

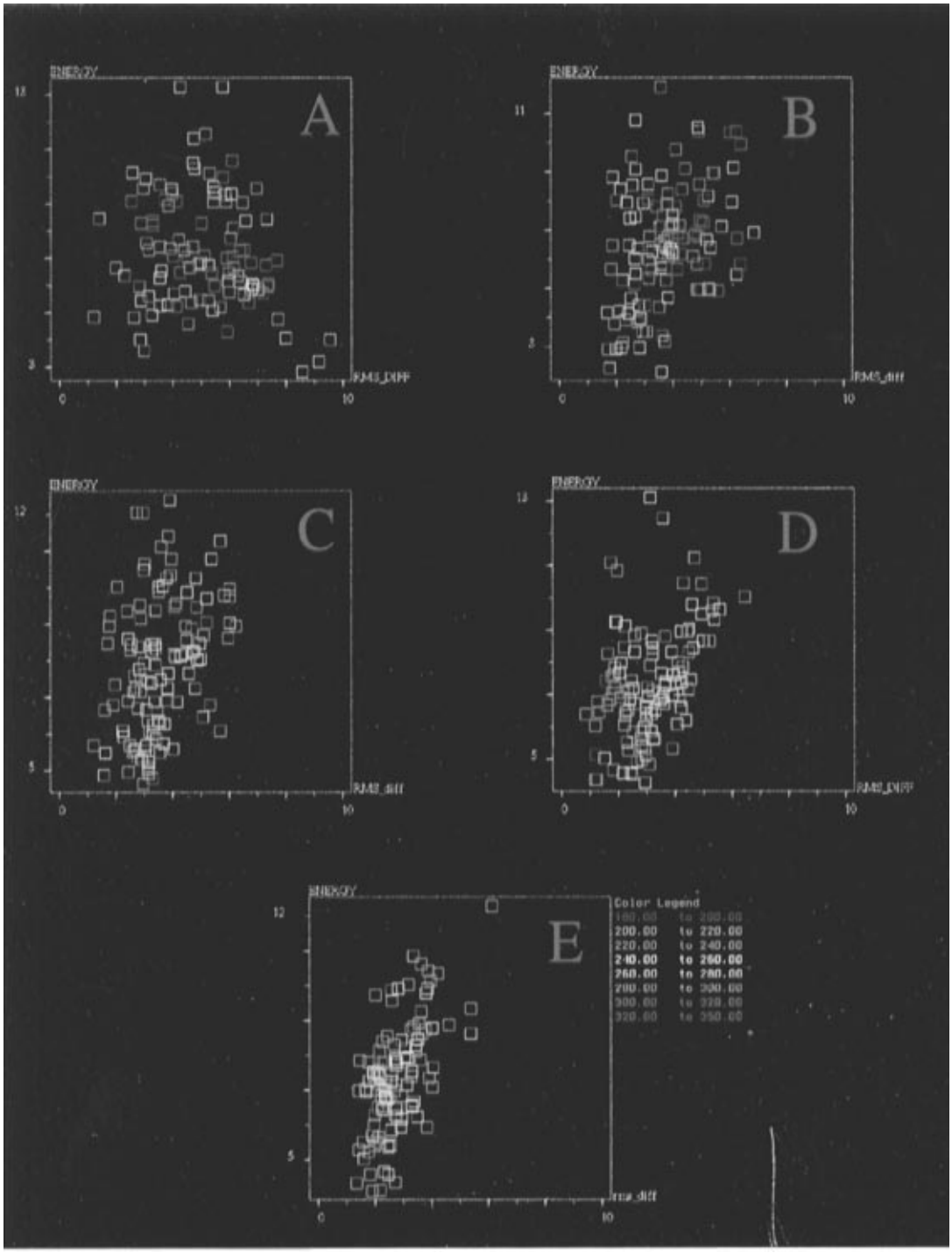

Figure 3. Graphs comparing the conformational freedom of anandamide analogs with varying degrees of unsaturation (A = 0 in arachidic acid, B = 1 in 11-eicosaenoic acid ethanolamide, C = 3 in 8,11,14-homo-γ-linolenylic acid ethanolamide, D = 4 (anandamide), and E = 5 in 5,8,11,14,17-eicosapentaenoic acid ethanolamide) and their ability to overlay with Δ^9-THC. The rms deviation (Å) from the five-point overlap is plotted on the *x*-axis, the energy (kcal/mol) of each conformation is plotted on the *y*-axis, and the extent of nonoverlapping volume (Å^3) is indicated by the color coding.

damide; Figure 3D), and finally to the most concentrated pattern of points obtained with the analog with five double bonds (eicosapentaenoic acid ethanolamide; Figure 3E). Furthermore, the difference between the molecular volume of Δ^9-THC and a particular analog also decreases as the number of double bonds increases, reaching a minimum volume difference at four double bonds, as indicated by the color coding. The absolute best volume overlap (purple symbol, 180−200 Å^3) between the various fatty acids with Δ^9-THC occurs *only* at the tetraene level. Beyond four double bonds the rms deviations appear to continue to decrease; however, the volume difference begins to increase again. Therefore, even though the range and magnitude of the rms deviation continued to decrease in the conformations obtained with five double bonds, the *optimal combination of all three factors appears to be at four double bonds* (i.e., the structure of anandamide).

One could hypothesize that the difference in the proportions of different conformations among these analogs (the conformational equilibria) will be related to their relative potency. In fact, among the five fatty

Table 1. Behavioral Potency, Energy, and Superposition of Tetraene Analogs Constrained to Pharmacophore Alignment

compound	ED_{50} (μmol/kg) spontaneous activity[a]	ED_{50} (μmol/kg) tail-flick latency[a]	pharmacophore overlay energy[b] (kcal/mol)	global minimum energy[c] (kcal/mol)	rms deviation[d] (Å)	volume difference[e] (Å^3)
anandamide (arachidonic acid ethanolamide)	50.3	17.4	5.7	4.3	1.3	152
arachidonic acid propanolamide	43.7	61.4	3.8	−0.4[f]	1.0	164
arachidonic acid pentanolamide	49.5	72.9	5.4	2.0	0.8	186
arachidonic acid phenyl ether ethanolamide	23.0	74.1	2.9	−1.0	1.8	219
arachidonic acid methyl ether ethanolamide	186.1	ND[g]	6.1	2.8	2.7	182
arachidonic acid 2′-fluoroethylamide	57.2	190.0	3.3	1.2	1.0	148
arachidonic acid 2,2-dimethylethanolamide	30.5	49.6	11.7	8.6	1.7	173
arachidonic acid morpholinoamide	20.7	25.4	4.9	3.6	0.9	168

[a] Pharmacological potency taken from Adams et al., 1995. [b] Energy of analogs that were initially constrained to pharmacophore alignment during energy minimization. [c] Minimum energy conformation obtained by quenched molecular dynamics simulations at 500 K. [d] rms deviation between conformation obtained when constrained to pharmacophore alignment and Δ^9-THC. [e] Volume difference between conformation obtained when constrained to pharmacophore alignment and Δ^9-THC. [f] Minimum energy conformation had intramolecular hydrogen bond (non-hydrogen bonded minimum energy conformation was 2.6 kcal/mol). [g] Potency was not able to be determined (>276 μmol/kg).

acid ethanolamides, anandamide, eicosapentaenoic acid ethanolamide, and homo-γ-linolenylic acid ethanolamide possess some affinity for the cannabinoid receptor[1,8,6] and also favor conformations which can be superposed with Δ^9-THC, whereas arachidic acid and 11-eicosaenoic acid ethanolamide do not. Although this is a qualitative observation, this datum does support the relevance of the proposed pharmacophore conformation.

Constraint of Tetraene Anandamide Analogs to Pharmacophoric Conformations. In the anandamide analogs that maintain a constant tetraene chain, their ability to align the five superposition points is not compromised by the presence of various substituents at the amide terminus (data not shown). Even the morpholino and phenyl ether analogs can achieve conformations that permit reasonable atom to atom overlap (i.e., low rms deviation). By constraining these analogs to maximize their similarity to the overlap to Δ^9-THC postulated for anandamide, and then minimizing their structure while gradually removing these constraints, it was found that reasonable pharmacophore overlap structures could be obtained at energies that were within 5 kcal of the global energy minimum as determined by the molecular dynamics simulations (Table 1).

Prediction of the Pharmacological Potencies of Tetraene Anandamide Analogs. As indicated previously, by gradually releasing the conformational restraints, it was possible to maintain enough structural similarity within the tetraene analogs so that quantitative structure−activity analyses could be performed using CoMFA. The in vivo behavioral potencies of these eight tetraene anandamide analogs could be predicted with a reasonable degree of accuracy *using a QSAR model based solely on classical and nonclassical cannabinoids*. Correlation coefficients of 0.54 ($P = 0.1$) and 0.37 ($P = 0.4$) were obtained between predicted and actual potencies in the spontaneous activity and tail-flick assays, respectively (Figure 4).

Rederivation of the CoMFA QSAR Model after Inclusion of Tetraene Anandamide Analogs. The ability of the QSAR analysis to accommodate the anandamide analogs was tested by PLS analysis with and without cross-validation. The cross-validated r^2 and the final r^2 values, determined for each experimental condition, are provided in Table 2. The r^2 values are also provided for analyses performed without inclusion of the anandamide, in order to evaluate the effect of the

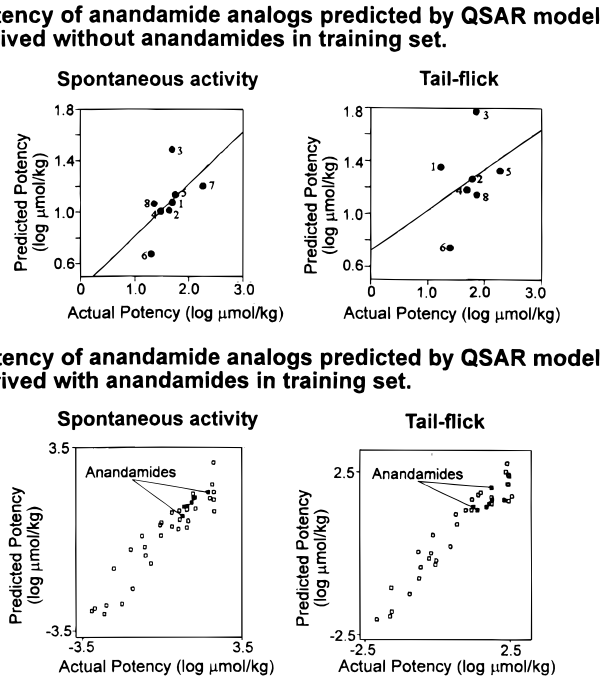

Figure 4. Correlation between predicted and actual potencies of tetraene anandamide analogs. Predicted ED_{50} values of anandamide analogs to decrease spontaneous locomotor activity and tail-flick latency are plotted against their actual ED_{50} values. The top graphs are obtained when predictions are made solely on the basis of classical and nonclassical cannabinoids (i.e., no anandamide analogs in training set): 1 = anandamide, 2 = arachidonic acid propanolamide, 3 = arachidonic acid pentanolamide, 4 = arachidonic acid 2,2-dimethylethanolamide, 5 = arachidonic acid 2′-fluoroethylamide, 6 = arachidonic acid morpholinoamide, 7 = arachidonic acid methyl ether ethanolamide, 8 = arachidonic acid phenyl ether ethanolamide. The lower graphs show the prediction of the anandamide analogs (solid symbols) when they are included in the training set of classical and nonclassical cannabinoids (open symbols).

anandamide analogs on the QSAR analyses. Although some differences can be noted between analyses, the inclusion of the anandamide analogs and the rederivation of the QSAR model did not appear to adversely affect its accuracy for predicting behavioral potency (Figure 4).

Comparison of CoMFA Fields. Plotting the CoMFA results contoured according to their PLS contribution enables visualization of important steric and electrostatic regions that are correlated with experimentally determined differences in behavioral potency. As one

Table 2. Cross-Validated and Final r^2 Values for QSAR Analyses[a]

QSAR analysis	optimal no. of components	r^2 cross-validated	r^2 final	standard error	*F* value
ability to fit the ED_{50} values for inhibition of spontaneous acitivity using leave-one-out cross-validation process (model derived *without* anandamides, total number of compounds = 33)	4	0.63	0.92	0.43	86
ability to fit the ED_{50} values for inhibition of spontaneous acitivity using leave-one-out cross-validation process with anandamides (model derived *with* anandamides, total number of compounds = 41)	3	0.62	0.90	0.45	116
ability to fit the ED_{50} values for tail-flick inhibition using leave-one-out cross-validation process (model derived *without* anandamides, total number of compounds = 33)	4	0.45	0.89	0.50	58
ability to fit the ED_{50} values for tail-flick inhibition using leave-one-out cross-validation process with anandamides (model derived *with* anandamides, total number of compounds = 41)	5	0.45	0.93	0.40	85

[a] The cross-validated (leave-one-out) r^2 values are provided along with the final r^2 values obtained with an equation set to the optimal number of components.

would expect, the results derived based on classical and nonclassical cannabinoids using a 1 Å grid spacing were similar to the results obtained in our original analyses based on a 2 Å spacing (data not shown, see ref 15 for complete description). However, when the PLS analysis was rederived with the eight anandamide analogs included, the steric and electrostatic plots still revealed only minor changes. Specifically, when examining the steric plots, one could see that a region where decreased predicted potency is associated with steric bulk behind the plane of the aromatic ring at the C11 position of Δ^9-THC had changed slightly. This area corresponds to the volume occupied by the inactive isomers of classical and nonclassical compounds and is only slightly extended after the inclusion of the anandamide analogs. Anandamide analogs whose steric bulk would penetrate into this region include the propanolamide and pentanolamide analogs. Areas indicating where steric bulk is associated with increased predicted potency also appeared to be only marginally affected by the inclusion of the anandamide analogs. Similarly, the electrostatic maps, when generated with and without inclusion of the anandamide analogs, were extremely similar. Thus, as the cross-validation runs had indicated, the pharmacophore models for pharmacological potency in the spontaneous activity and tail-flick assays of cannabimimetic activity appear to be able to accommodate the anandamide analogs into the training set without dramatically altering the QSAR analyses.

Discussion

The dynamics simulations used in this study have previously been shown (with arachidonic acid and other fatty acids) to accurately evaluate conformational mobility.[19] In this research on fatty acids, Rich demonstrated that simulations of arachidonic acid, linoleic acid, oleic acid, and arachidic acid at 500 K provided the most thorough conformational sampling. Furthermore, it was shown that simulations for 1000 ps did not increase the number of low-energy conformations as compared to those obtained in simulations lasting 100 ps. In the present study, a three-dimensional structure of anandamide was obtained through dynamics simulations at 500 K and subsequently used to establish a hypothetical alignment with Δ^9-THC. This three-dimensional structure of anandamide is in agreement with the conformational studies of arachidonic acid[19] and the chemistry of arachidonic acid as noted by Corey and colleagues.[20] This conformation possesses (1) a low RMS deviation from Δ^9-THC, (2) the greatest volume overlap with Δ^9-THC, and (3) a relatively low conformational energy (<2 kcal/mol above global minimum energy). The rationale for its selection as a putative pharmacophoric conformation involved a number of criteria, including its ability to align key electronegative atoms and hydrocarbon side chains with Δ^9-THC while maximizing their overlap with respect to molecular volume. In this conformation, the degree of steric overlap and electrostatic similarity between anandamide and Δ^9-THC is relatively high. Indeed, the similarity in its steric and electrostatic properties with those of Δ^9-THC is such that it is correctly predicted to possess pharmacological activity by our original CoMFA QSAR study[15] based on 33 classical and nonclassical compounds (predicted ED_{50} in inhibiting spontaneous locomotor activity in mice of 11.6 μmol/kg vs actual ED_{50} of 50.3 μmol/kg; predicted ED_{50} in increasing tail-flick latency in mice of 22.4 μmol/kg vs actual ED_{50} of 17.4 μmol/kg).

The molecular dynamics simulations also indicate whether a particular anandamide analog can achieve a conformation that allows the alignment of key atoms within our hypothesized pharmacophore overlay. By comparing a number of anandamide analogs with differing degrees of unsaturations, we have shown that: (1) the number of double bonds can affect their ability to overlay with Δ^9-THC, (2) that as their ability to overlay specific atoms with Δ^9-THC increases, pharmacological potency also increases, and (3) at five double bonds, the restricted conformational mobility, although still allowing atom to atom overlap, appears to compromise its ability to maximize volume overlap. Therefore, there appears to be a correlation, although qualitative, between the ability to attain a pharmacophoric conformation and pharmacological potency.

Interestingly, all of the tetraene analogs that have been investigated have been able to fit to Δ^9-THC with a low rms deviation, even the phenyl ether and morpholino analogs. Since all of the tetraene anandamide analogs have been reported to bind with reasonable affinity to the cannabinoid receptor, or produce cannabimimetic activity in mice,[6] the ability of these analogs to achieve similar overlaying conformations supports the proposed pharmacophoric alignment of anandamide and anandamide analogs to Δ^9-THC. Furthermore, the ability to predict the potency of these

compounds, which represent a structural class of compounds entirely different from those on which the initial model is based and also possess a limited range of pharmacological potencies (ca. 1 log unit as compared to a model based on a dynamic range of 5 log units), provides quantitative support for this pharmacophoric alignment. Although the correlation coefficients of 0.54 and 0.37 are not statistically significant, the ability to correctly indicate a potency trend for compounds possessing structural variations which are not represented by some of the entries in the training set is extremely difficult.[23] This is particularly the case when transport, distribution, and metabolism within the biological test system may be quite different between the anandamides and the classical and nonclassical cannabinoids. Finally, the validity of the proposed pharmacophore model is substantiated by its ability to include the anandamide analogs into the previously derived QSAR without compromising the accuracy of the model's predictions or altering the shape of the CoMFA-derived pharmacophores.

Although previous molecular modeling studies support the existence of a pharmacophore that can accommodate classical and nonclassical cannabinoids[13−15,24,25] as well as the aminoalkylindoles,[26,15] the ability to also include anandamide analogs had not been tested. Indeed, due to the anandamides' relatively unconstrained conformational freedom, the identification of a "relevant" alignment with fatty acid ethanolamides has proven to be particularly difficult. However, the pharmacophore model described by CoMFA is consistent with the behavioral data thus far obtained for anandamide and its analogs,[6,10] which suggests the presence of an active site, or overlapping binding sites, on the cannabinoid receptor that can accommodate a wide variety of cannabinoid analogs.

It should be emphasized that the proposed pharmacophore alignment of fatty acid ethanolamides and classical cannabinoids should not be interpreted as indicating an exact atom to atom overlap or a mapping of structurally-required features for these two distinct classes of compounds. For example, the *N*-propylarachidonylamide analog synthesized and tested by Pinto et al. in 1994,[9] despite the substitution of the hydroxyl group with a methyl, possesses a 3-fold greater affinity for the cannabinoid (CB1) receptor. This is unusual in that classical and nonclassical cannabinoids typically show reduced affinity for the CB1 receptor and decreased biological potency when the phenolic hydroxyl is replaced with a hydrogen.[27] A plausible explanation for the apparent activity of this compound is that it possesses additional functionality that compensates for the absence of the hydroxyl group. In addition, the question remains as to whether the decrease in potency in classical and nonclassical cannabinoids that occurs with the removal of the hydroxyl is due to the removal of an electrostatic region, the absence of a region of steric bulk (which would not be the case in *N*-propylarachidonylamide), or a combination of these features. Unfortunately, the *N*-propylarachidonylamide compound has not been tested in the behavioral paradigms we are modeling. Nevertheless, the proposed alignment represents a theoretical framework allowing rational structural comparison between the fatty acid ethanolamides and other cannabimimetics. Since the model possesses predictive power, future extension of this work will include prediction of candidate compounds for synthesis and further development of our pharmacophore model to include the wide variety of cannabinoid agonists (and antagonists) that have been described.

References

(1) Devane, W. A.; Hanus, L.; Breuer, A.; Pertwee, R. G.; Stevenson, L. A.; Griffin, G.; Gibson, D.; Mandelbaum, A.; Etinger, A.; Mechoulam, R. Isolation and Structure of a Brain Constituent That Binds to the Cannabinoid Receptor. *Science* **1992**, *258*, 1946−1949.

(2) Vogel, Z.; Barg, J.; Levy, R.; Saya, D.; Heldman, E.; Mechoulam, R. Anandamide, a Brain Endogenous Compound, Interacts Specifically with Cannabinoid Receptors and Inhibits Adenylate Cyclase. *J. Neurochem.* **1993**, *61*, 352−355.

(3) Felder, C. C.; Briley, E. M.; Axelrod, J.; Simon, J. T.; Mackie, K.; Devane, W. A. Anandamide, an Endogenous Cannabimimetic Eicosanoid, Binds to the Cloned Human Cannabinoid Receptor and Stimulates Receptor-Mediated Signal Transduction. *PNAS* **1993**, *90*, 7656−7660.

(4) Fride, E.; Mechoulam, R. Pharmacological Activity of the Cannabinoid Receptor Agonist, Anandamide, a Brain Constituent. *Eur. J. Pharmacol.* **1993**, *231*, 313−314.

(5) Smith, P. B.; Compton, D. R.; Welch, S. P.; Razdan, R. K.; Mechoulam, R.; Martin, B. R. The Pharmacological Activity of Anandamide, a Putative Endogenous Cannabinoid, in Mice. *J. Pharmacol. Exp. Ther.* **1994**, *270*, 219−227.

(6) Adams, I. B.; Ryan, W.; Singer, M.; Thomas, B. F.; Compton, D. R.; Razdan, R. K.; Martin, B. R. Evaluation of Cannabinoid Receptor Binding and In-Vivo Activities for Anandamide Analogs. *J. Pharmacol. Exp. Ther.* **1995**, *273*, 1172−1181.

(7) Crawley, J. N.; Corwin, R. L.; Robinson, J. K.; Felder, C. C.; Devane, W. A.; Axelrod, J. Anandamide, an Endogenous Ligand of the Cannabinoid Receptor, Induces Hypomotility and Hypothermia In Vivo in Rodents. *Pharmacol. Biochem. Behav.* **1993**, *46*, 967−972.

(8) Hanus, L.; Gopher, A.; Almog, S.; Mechoulam, R. Two New Unsaturated Fatty Acid Ethanolamides in Brain that Bind to the Cannabinoid Receptor. *J. Med. Chem.* **1993**, *36*, 3032−3034.

(9) Pinto J. C.; Potie, F.; Rice, K. C.; Boring, D.; Johnson, M. R.; Evans, D. M.; Wilkin, G. H.; Cantrell, C. H.; Howlett, A. C. Cannabinoid Receptor Binding and Agonist Activity of Amides and Esters of Arachidonic Acid. *Mol. Pharm*acol. **1994**, *46*, 516−522.

(10) Abadji, V.; Lin, S.; Taha, G.; Griffin, G.; Stevenson, L. A.; Pertwee, R. G.; Makriyannis, A. (R)-Methanandamide: a Chiral Novel Anandamide Possessing Higher Potency and Metabolic Stability. *J. Med. Chem.* **1994**, *37*,1889−1893.

(11) Binder, M.; Franke I. Is there a Cannabinoid Receptor? Current Perspectives and Approaches to the Elucidation of the Molecular Mechanism of Action of the Psychotropic Constituents of *Cannabis sativa L.* In *Neuroreceptors;* Hucho, F., Ed.; Walter de Gruyter: Berlin, 1982; pp 151−161.

(12) Razdan, R. K. Structure-Activity Relationships in the Cannabinoids. *Pharm. Rev.* **1986**, *38*, 75−149.

(13) Reggio, P. H.; Greer, K. W.; Cox, S. M. The Importance of the Orientation of the C9 Substituent to Cannabinoid Activity. *J. Med. Chem.* **1989**, *32*, 1630−1635.

(14) Kriwacki, R. W.; Makriyannis, A. The Conformational Analysis of Δ^9- and $\Delta^{9,11}$-Tetrahydrocannabinols in Solution using High Resolution Nuclear Magnetic Resonance Spectroscopy. *Mol. Pharmacol.* **1989**, *35*, 495−503.

(15) Thomas, B. F.; Compton, D. R.; Martin, B. R.; Semus, S. F. Modeling the Cannabinoid Receptor: A Three-Dimensional Quantitative Structure-Activity Analysis. *Mol. Pharmacol.* **1991**, *40*, 656−665.

(16) Milne, G. M.; Johnson, M. R. Levonantradol: a Role for Central Prostanoid Mechanisms. *J. Clin, Pharmacol.* **1981**, *21*, 367S.

(17) Johnson, M. R.; Melvin, L. S. The Discovery of Nonclassical Cannabinoid Analgetics. In *Cannabinoids as Therapeutic Agents*; CRC Press: Boca Raton, FL, 1986; pp 121−145.

(18) Devane, W. A.; Dysarz, F. A.; Johnson, M. R.; Melvin, L. S.; Howlett, A. C. Determination and Characterization of a Cannabinoid Receptor in Rat Brain. *Mol. Pharmacol.* **1988**, *34*, 605−613.

(19) Rich, M. R. Conformational Analysis of Arachidonic and Related Fatty Acids using Molecular Dynamics Simulations. *Biochim. Biophys. Acta* **1993**, *1178*, 87−96.

(20) Corey, E. J.; Niwa, H.; Falck, J. R. Selective Epoxidation of Eicosa-cis 5,8,11,14-tetraenoic (Arachidonic) Acid and Eicosa-cis-8,11,14-trienoic Acid. *J. Am. Chem. Soc.* **1979**, *101*, 1586−1587.

(21) Corey, E. J.; Iguchi, S.; Albright, J. O.; De, B. Studies on the Conformational Mobility of Arachidonic Acid: Facile Macrolactonization of 20-Hydroxyarachidonic Acid. *Tetrahedron Lett.* **1983**, *24*, 37.

(22) Reggio, P. H. Molecular Determinants of Cannabinoid Activity: Toward the Design of Cannabinoid Analgesics with Reduced Psychoactive Liability. *Natl. Inst. Drug Abuse Res. Monogr.* **1993**, *134*, 210−228.
(23) Thibaut, U.; Folkers, G.; Klebe, G.; Kubinyi, H.; Merz, A.; Rognan, D. Recommendations for CoMFA Studies and 3D QSAR Publications. In *3D QSAR in Drug Design*: *Theory, Methods and Applications*; Kubinyi, H., Ed., ESCOM: Leiden, 1993; pp 711−716.
(24) Melvin, L. S.; Johnson, M. R.; Harbert, C. A.; Milne, G. M.; Weissman, A. A Cannabinoid Derived Prototypical Analgesic. *J. Med. Chem.* **1984**, *27*, 67−71.
(25) Reggio, P. H. Molecular Determinants for Cannabinoid Activity: Refinement of a Molecular Reactivity Template. *Natl. Inst. Drug Abuse Res. Monogr.* **1987**, *79*, 82−95.
(26) Huffman, J. W.; Dai, D. Design, Synthesis and Pharmacology of Cannabimimetic Indoles. *Biomed. Chem. Lett.* **1994**, *4*, 563−566.
(27) Melvin, L. S.; Milne, G. M.; Johnson, M. R.; Subramaniam, B.; Wilken, G. H.; Howlett, A. C. Structure-Activity Relationships for Cannabinoid Receptor-Binding and Analgesic Activity: Studies of Bicyclic Cannabinoid Analogs. *Mol. Pharmacol.* **1993**, *44*, 1008−1015.

JM9505167